Received: 12 December 2019 | Revised: 10 March 2020 | Accepted: 26 March 2020

DOI: 10.1111/ffe.13242

ORIGINAL CONTRIBUTION

FFEMS Fatigue & Fracture of Engineering Materials & Structures WILEY

Scaling and fractality in fatigue resistance: Specimen-size effects on Wöhler's curve and fatigue limit

Alberto Carpinteri | **Francesco Montagnoli** | **Stefano Invernizzi**

Department of Structural, Geotechnical and Building Engineering, Politecnico di Torino, Torino, Italy

Correspondence
Department of Structural, Geotechnical and Building Engineering, Politecnico di Torino, Corso Duca degli Abruzzi 24, 10129 Torino, Italy.
Email: francesco.montagnoli@polito.it

Abstract

The present contribution investigates size effects on Wöhler's curve in accordance with dimensional analysis and intermediate asymptotics theory. These approaches provide a generalised equation able to interpret the specimen-size effects on Wöhler's curve. Subsequently, using a different approach based on lacunar fractality concepts, analogous scaling laws are found for the coordinates of the limit-points of Wöhler's curve, so that a theoretical explanation is provided to the decrement in fatigue resistance by increasing the specimen size. Eventually, the proposed models are compared with experimental data available in the Literature, which seem to confirm the advantage of applying fractal geometry to the problem.

KEYWORDS

dimensional analysis, fatigue limit, fractal geometry, intermediate asymptotics, size-scale effects, Wöhler's curve

1 | INTRODUCTION

Fatigue failure represents one of the most common causes of collapse of industrial and civil structures, where more than 90% of failures can be considered as the result of this phenomenon. The first research on the fatigue problem was carried out by Wöhler,[1] who performed a series of experimental tests on unnotched steel specimens subjected to cyclic loading. This *modus operandi* permitted the determination of the number of cycles to failure as a function of the applied stress range, $\Delta\sigma$, which, through the best fitting of the experimental data, allowed to obtain the so-called Wöhler's curve.

In this empirical S-N curve, it is possible to distinguish three different regions. In the first one, the failure occurs for low numbers of cycles with considerable plastic deformations, and the Coffin-Manson relationship holds. On the other hand, in the high-cycle fatigue region, plastic deformations become negligible, and a power-law approximation can be used, that is, the so-called Basquin's law[2]:

$$\Delta\sigma = \frac{\Delta\sigma_0}{N^{1/n}}. \tag{1}$$

The latter represents the equation of a straight line in the bi-logarithmic diagram, where $1/n$ is the slope, whereas $\Delta\sigma_0$ is the intercept. The transition between the low-cycle fatigue regime and the Basquin's regime is defined by the limit-point A, which is the intersection between the horizontal line of stress range at static failure $\Delta\sigma_{cr}$ and the Basquin's straight line in the bi-logarithmic diagram. The x-coordinate of the point A is equal to N_{cr}, which ranges between 10^3 and 10^4 cycles.[3] Eventually, the third region corresponds to the so-called infinite-life region, where a constant fatigue limit, $\Delta\sigma_{fl}$, is attained. The existence and value of $\Delta\sigma_{fl}$ is still debated for different materials and applications. The transition between Basquin's regime and infinite-life region is defined by point B. The x-coordinate of point B, (N_{fl} in Figure 1), is conventionally assumed equal to 10^7 cycles.

According to Moore and Harter,[4] the first experimental detection of the size effects in fatigue dates back to 1930. The first quantitative interpretation was obtained a

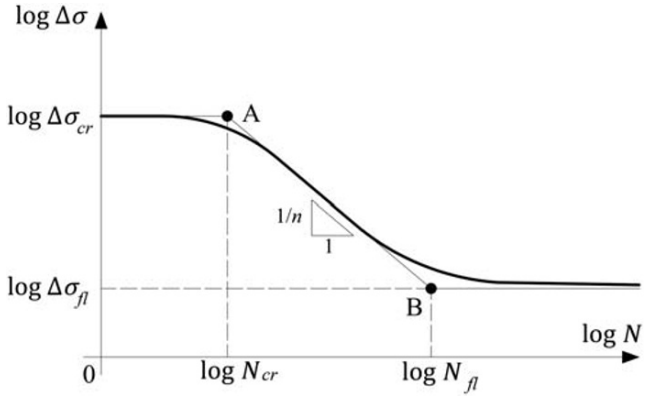

FIGURE 1 Wöhler's curve

decade later on the basis of statistical theories.[5] In the 1980s, some researchers provided alternative formulations exploiting intermediate asymptotics theory.[6] In addition, Murakami determined experimentally a relationship between the fatigue limit and the defect of maximum size, the so-called $\sqrt{area}$ model[7–9]:

$$\Delta\sigma_{fl} = \frac{1.56(HV + 120)}{(\sqrt{area})^{1/6}}, \tag{2}$$

where $\sqrt{area}$ is the square root of the area of the defect of maximum size projected onto a plane orthogonal to the maximum tensile stress and is measured in micrometres, *HV* being the Vickers hardness of the material. The maximum size of the inclusion, embedded in the risk volume, can be estimated by extreme value statistics,[10] once that the distribution of defects in the standard inspection volume has been experimentally assessed. The risk volume is usually defined as the region where the stress is higher than the 90% of the peak value.

Murakami et al. noted also that, when a specimen fails in ultralong life regime, the fatigue fracture does not originate from the surface but near an internal inclusion, which can be clearly identified by fractography, thanks to the so-called fish-eye morphology, and by the surrounding Optically Dark Area (ODA).[11,12]

Since the development of ultrasonic fatigue testing machines, working at a very high frequency and allowing for very high number of cycles tests in a relatively short time, the interest of the scientific community about the size effects on the fatigue limit has increased.[13,14] Furuya[15] performed ultrasonic fatigue tests on a high-strength steel and assessed the size-effect on the fatigue limit according to Equation 2, which states that the larger the risk volume, the lower the fatigue limit.

Tridello et al.[16–20], in order to investigate the statistical size effect on the fatigue strength, designed an innovative specimen shape with Gaussian profile, which can be used to enlarge the risk volume of the specimen. Therefore, they were able to test a high-strength steel, AISI H13, and to analyse results from a wide range of different risk volumes.

Decades ago, the concept of fractality was exploited by Carpinteri[21] to explain the size effect on Linear Elastic Fracture Mechanics parameters. In this framework, the material disorder due to the presence of a distribution of flaws, inclusions, and micro-cracks is accounted for adopting a fractal, rather than Euclidean, geometrical model. In this way, the statistical population of defects is replaced by a fractal medium, which is populated of defects and lacunarities at each scale of observation. Following this approach, Carpinteri et al.[22] provided an expression for the experimentally observed specimen-size effects on Basquin's law.

The purpose of the present paper is to apply the concepts of dimensional analysis and incomplete self-similarity to Wöhler's curve so that the different functional dependencies of the fatigue life can be considered through a power-law expression. Subsequently, by modelling the reacting section as a lacunar fractal domain with a noninteger dimension, which is lower than 2, it is possible to confirm the specimen-size dependence of Wöhler's curve, which is experimentally found in the Literature. Moreover, in order to model the variation of the fatigue limit over a wide size range, a Multi-Fractal Scaling Law (MFSL) is proposed for this parameter. Eventually, the proposed models are compared with experimental data available in the Literature, which seem to confirm the advantage of applying a fractal model to the specimen-size effect on Wöhler's curve.

2 | INTERMEDIATE ASYMPTOTICS APPLIED TO WÖHLER'S CURVE

In accordance with dimensional analysis, the following functional dependence can be considered for Wöhler's curve[23,24]:

$$N = \Pi\left(\Delta\sigma, 1-R; \sigma_u, K_{IC}, \Delta\sigma_{fl}; b\right), \tag{3}$$

where we assume that the number of cycles to failure, *N*, is the parameter to be determined. The latter is a function of three different categories of variables:

1 parameters that take into account the testing conditions, that is, the stress range, $\Delta\sigma$, and the loading ratio, *R*;
2 parameters that take into account the static and cyclic material properties, such as the ultimate tensile stress,

σ_u, the fracture toughness, K_{IC}, and the fatigue limit, $\Delta\sigma_{fl}$;
3 the geometric parameter, that is, the characteristic specimen size b.

Actually, we are neglecting the dependence on the time, that is, on the frequency. The physical dimensions of the parameters in Equation 3 are expressed in the Length-Force-Time class:

$$N = 1-R = [-],\ K_{IC} = [\mathrm{F}][\mathrm{L}]^{-\frac{3}{2}},\ \Delta\sigma = \Delta\sigma_{fl} = \sigma_u = [\mathrm{F}][\mathrm{L}]^{-2},\ b = [\mathrm{L}].$$

From dimensional analysis,[25] because only two quantities are dimensionally independent, the number of parameters involved in the problem could be reduced from six to four, so that Equation 3 becomes

$$N = \bar{\Pi}\left(\frac{\Delta\sigma}{\sigma_u}, 1-R; \frac{\Delta\sigma_{fl}}{\sigma_u}; \frac{{\sigma_u}^2}{{K_{IC}}^2} b\right), \tag{4}$$

where the following dimensionless parameters have been introduced:

$$\Pi_1 = \frac{\Delta\sigma}{\sigma_u},\ \Pi_2 = 1-R;\ \Pi_3 = \frac{\Delta\sigma_{fl}}{\sigma_u};\ \Pi_4 = \left(\frac{\sigma_u}{K_{IC}}\right)^2 b.$$

Let us observe that Π_4 is responsible for the specimen-size dependence of the fatigue behaviour. In fact, the latter is equal to the inverse of the square of the brittleness number, s.[26]

The intermediate asymptotics theory allows us further reduce the number of quantities involved in Equation 4.[27–30] To this aim, let us assume an incomplete self-similarity in the dimensionless parameters Π_i, so that a power-law dependence of the number of cycles, N, on Π_i can be obtained:

$$N = \left(\frac{\Delta\sigma}{\sigma_u}\right)^{\alpha_1} (1-R)^{\alpha_2} \left(\frac{\Delta\sigma_{fl}}{\sigma_u}\right)^{\alpha_3} \left(\frac{{\sigma_u}^2}{{K_{IC}}^2} b\right)^{\alpha_4}. \tag{5}$$

Therefore, in Equation 5, the main functional dependencies of N have been considered so that a generalised Wöhler's relationship is obtained. For instance, the S-N curve can be approximated by the Basquin power-law for high-cycle fatigue:

$$N_{cr} \times \Delta\sigma_{cr}^n = N \times \Delta\sigma^n = 1 \times \Delta\sigma_0^n = \text{constant}. \tag{6}$$

Hence, by matching the left-hand side of Equation 6 with the right-hand side, we can write the following power-law:

$$N = N_{cr}\left(\frac{\Delta\sigma_{cr}}{\Delta\sigma}\right)^n. \tag{7}$$

Furthermore, considering the relationship between ultimate tensile strength and loading ratio:

$$\Delta\sigma_{cr} = (1-R)\,\sigma_u, \tag{8}$$

we obtain the expression that relates the number of cycles to failure to the stress range:

$$N \propto \frac{(1-R)^n\ {\sigma_u}^n}{\Delta\sigma^n}. \tag{9}$$

Comparing the generalised expression of the S-N curve in Equation 5 with the empirical one in Equation 9, a perfect correspondence between them exists if:

$$\alpha_1 = -n, \qquad \alpha_2 = -n, \tag{10a}$$

$$\alpha_3 = \alpha_4 = 0, \tag{10b}$$

which implies an incomplete self-similarity in Π_1 and Π_2 and a complete self-similarity in Π_3 and Π_4, that is, Basquin's law does not take into account the size effects.

3 | SOME REMARKS ON THE LACUNAR FRACTALITY AND MULTI-FRACTALITY

In the last few decades, it has been widely recognised that the nominal tensile strength is not a material constant, but rather, it depends on the structural size. As a matter of fact, the ultimate strength of a material decreases with the specimen size, and this trend is more pronounced for more disordered materials.[21] In other words, the reacting section or ligament of a disordered material can be modelled as a fractal set, where its noninteger dimension lower than 2 is the way to quantify the disorder itself.[31] Thus, supposing that the total force is transmitted through a lacunar fractal ligament of dimension $\alpha = 2 - d_\sigma$, with $1 \le \alpha \le 2$, the following scaling law for nominal tensile strength can be proved[32–35]:

$$\sigma_u = \sigma_u^* b^{-d_\sigma}, \tag{11}$$

where σ_u^* is the scale-invariant tensile strength with noninteger physical dimensions $[\mathrm{F}][\mathrm{L}]^{-(2-d_\sigma)}$, whereas d_σ is the dimensional decrement of the ligament due to the

presence of cracks and voids distributions.[21,32] Eventually, Equation 11 can be written as:

$$\log\sigma_u = \log\sigma_u^* - d_\sigma \log b, \tag{12}$$

which represents the equation of a straight line in the bi-logarithmic diagram. Notice that the fractal dimension in Equation 11 is constant, so that we should talk about fractal scaling law. On the other hand, if we consider specimens with a very wide size range, the experimental results point out that a fractal scaling approach is valid only within a limited scale range, such that the fractal dimension can be really considered constant. This implies that, as the specimen size increases, the concept of geometrical multi-fractality should be put forward, that is, a change of d_σ with the scale of observation.[36–38]

This can be explained by recalling that the microstructure of a disordered material remains the same independently of the scale of observation. As a result, the influence of disorder on mechanical properties depends on the ratio between a characteristic material length, l_{ch}, and the characteristic size of the specimen, b. Hence, the effect of disordered nature on the mechanical parameters of the material turns out gradually less important for larger scales of observation, and, eventually, the fractality vanishes for b tending to infinity.

This transition from a disordered regime for smaller scales, where the fractal scaling exponent is equal to 1/2 due to a self-similar distribution of cracks, to an ordered regime for larger scales can, therefore, be considered for any mechanical quantity.[36] The analytical expression of the Multi-Fractal Scaling Law (MFSL) for tensile strength is the following (Figure 2)[39–41]:

$$\sigma_u(b) = \sigma_u^\infty \left(1 + \frac{l_{ch}}{b}\right)^{1/2}. \tag{13}$$

This scaling law represents a two-parameter best-fitting, where the asymptotic value of the ultimate strength, σ_u^∞, corresponding to its lowest value, is reached only in the limit case of infinite specimen sizes. Furthermore, the variable influence of disorder on tensile strength is represented by the dimensionless term within round brackets, which depends on the characteristic length l_{ch}. In other words, in the bi-logarithmic diagram, the transition from the fractal regime to the Euclidean one is represented by the point of asymptotes' intersection of abscissa $\log l_{ch}$, which is a function of the microstructure of the material.[42–44] The characteristic material length l_{ch} is a material property that can be proportional to the average defect size, or to the grain size, or to the inclusion size, depending on the mechanism responsible for fracture nucleation.

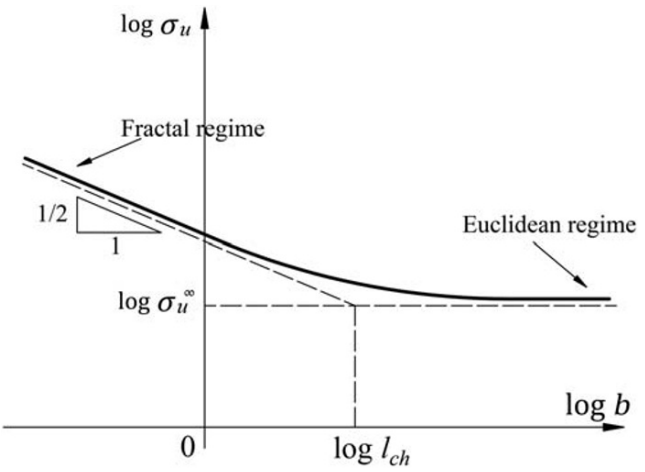

FIGURE 2 Size effect on ultimate tensile strength

4 | FRACTAL AND MULTI-FRACTAL APPROACH TO WÖHLER'S CURVE

As mentioned in Section 1, experimental evidences have pointed out a size effect on fatigue strength, which generally decreases with the specimen size. Although different interpretations able to give an explanation to the problem have been proposed in the Literature, such as Murakami's model, these consider only the maximum size defect, so neglecting the microstructural disorder of the material. Thus, by exploiting the renormalized quantities related to a lacunar fractal cross-section, the following scaling law for the stress range can be written[22,45]:

$$\Delta\sigma = \Delta\sigma^* b^{-d_\sigma}, \tag{14}$$

where the fractal stress range $\Delta\sigma^*$, with physical dimensions given by $[\mathrm{F}][\mathrm{L}]^{-(2-d_\sigma)}$, is considered invariant with respect to the scale of observation. Furthermore, because $0 \le d_\sigma \le 1$, Equation 14 predicts a decrement in the number of cycles to failure with the specimen size. On the other hand, considering the stress range as a function of N, Equation 14 predicts a decrease in $\Delta\sigma$ with the specimen size, N being the same. Thus, Equation 14 allows us to demonstrate that the fatigue strength undergoes size effects. It is worth noting that the assumption of the ligament lacunar fractality can be comprised in the intermediate asymptotics framework, when the dimensionless parameter $b\ {\sigma_u}^2/{K_{IC}}^2$ is provided with the noninteger exponent $\alpha_4 = -d_\sigma n$.

Similarly, the fractal approach can be used to explain the specimen-size effects on fatigue limit. In fact, because the fatigue limit is experimentally determined for a conventional very high number of cycles, Equation 14 can be evaluated in correspondence to the right knee-point of Wöhler's curve, that is, $N = N_{fl}$, so that the following scaling law for the fatigue limit is obtained:

$$\Delta\sigma_{fl} = \Delta\sigma^*_{fl} b^{-d_\sigma}, \tag{15}$$

where $\Delta\sigma^*_{fl}$ is the fractal fatigue limit, which is a material property with anomalous physical dimensions. Hence, Equation 15 provides the specimen-size effect on the fatigue limit. Indeed, in agreement with the concept of lacunar fractal set, we obtain a negative slope for the fatigue limit by varying the specimen size, that is, Equation 15 provides a decrement in $\Delta\sigma_{fl}$ with the specimen size. Eventually, Equation 15 can be written in the following form (Figure 3):

$$\log\Delta\sigma_{fl} = \log\Delta\sigma^*_{fl} - d_\sigma \log b, \tag{16}$$

which represents the equation of a straight line with slope equal to $-d_\sigma$ in a bi-logarithmic diagram.

Analogously, it is possible to define the specimen-size effect on the left knee-point of Wöhler's curve, that is, for $N = N_{cr}$. Thus, evaluating Equation 14 in correspondence of it, we obtain the following scaling law for the ordinate of the critical point:

$$\Delta\sigma_{cr} = \Delta\sigma^*_{cr} b^{-d_\sigma} = (1-R)\,\sigma^*_u\, b^{-d_\sigma}. \tag{17}$$

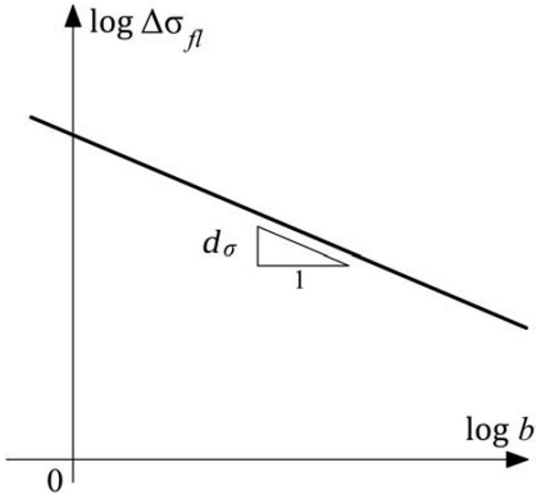

FIGURE 3 Specimen-size effects on fatigue limit in a bi-logarithmic diagram

Thus, Equations 15 and 17 yield a vertical downward translation of Wöhler's curve increasing the specimen size, that is, the larger the specimen dimension, the lower the fatigue strength. Thus, it is worth to note that, N_{cr} and N_{fl} being dimensionless parameters, only the vertical translation is expected (Figure 4), excluding the horizontal one.[46] On the other hand, substituting the nominal stress range with the corresponding fractal parameter, a fractal coordinate system is obtained, and a collapse of the set of specimen-size-dependent Wöhler's curves onto a single specimen-size-independent Wöhler's curve is expected (Figure 5).

Moreover, notice that, for $d_\sigma \to 1/2$, we obtain $\Delta\sigma_{fl} \propto b^{-1/2}$, so that the fractal fatigue limit assumes the physical dimensions of a stress-intensity factor, that is, $[F][L]^{-3/2}$.This observation implies that a value higher than 1/2 is not possible. In fact, this condition is obtained assuming a self-similar statistical size distribution such that the defect of maximum size is proportional to the structural size. As a result, this statement implies that the defect size distribution of self-similarity corresponds to the condition of maximum disorder. Hence, because the assumption of a self-similar statistical size distribution implies a value of the scaling exponent of strength versus structural size equal to 1/2, it follows that the maximum possible value for d_σ is 1/2.[32]

The next step concerns the introduction of the concept of self-affinity. In fact, although the decrease in fatigue limit by increasing the structural size can be obtained considering just the fractal approach, a Multi-Fractal Scaling Law for the fatigue limit should be put forward to capture the transition from the fractal regime to the Euclidean one:

$$\Delta\sigma_{fl} = \Delta\sigma^{\infty}_{fl}\left(1 + \frac{l_{ch}}{b}\right)^{1/2}. \tag{18}$$

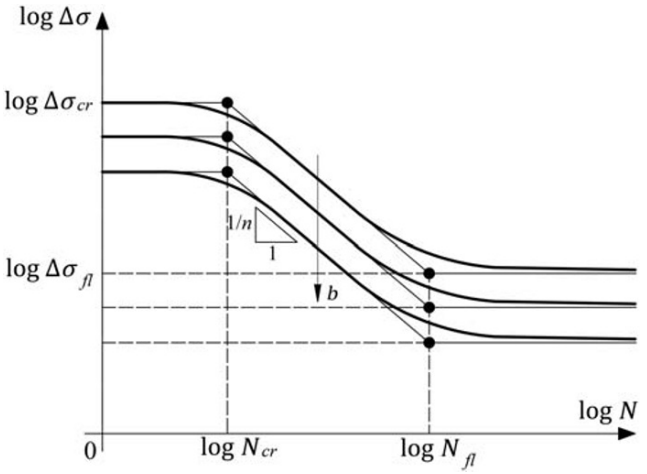

FIGURE 4 Specimen-size effects on Wöhler's curve

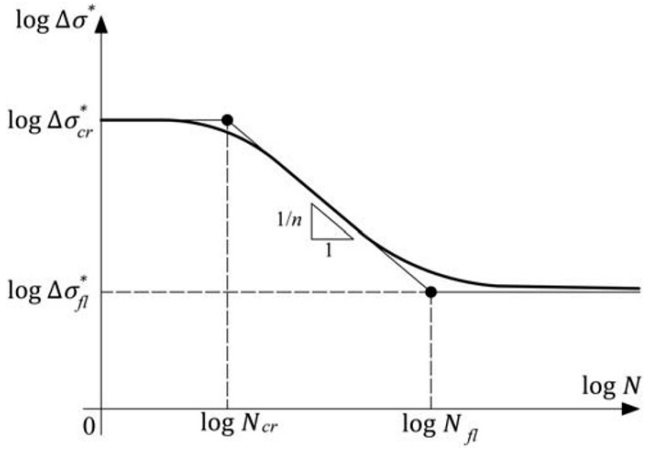

FIGURE 5 Fractal (specimen-size independent) Wöhler's curve

Thus, because a transition from disorder to the Euclidean order is expected for very large structural sizes, the fractal decrement, d_σ, tends to zero. Consequently, the specimen-size dependence of fatigue limit disappears, and we obtain its asymptotic value, $\Delta\sigma^{\infty}_{fl}$, which can be considered as a material constant. *Vice versa*, for very small specimens, the influence of the material disorder becomes progressively more important, and the fatigue limit increases as the specimen size decreases (see Figure 6). In other words, Equation 18 provides a decrement in the fatigue limit with the specimen size according to the assumption of a lacunar multi-fractal ligament.

The exponent of the term within round brackets represents the slope of the oblique asymptote in the bi-logarithmic diagram $\Delta\sigma_{fl}$ versus b, which is always lower than 1/2, as above mentioned. Furthermore, according to Equation 17, a Multi-Fractal Scaling Law for $\Delta\sigma_{cr}$ can be put forward to capture the transition from the fractal regime to the Euclidian one:

$$\Delta\sigma_{cr} = \Delta\sigma^{\infty}_{cr}\left(1+\frac{l_{ch}}{b}\right)^{1/2}, \tag{19}$$

where $\Delta\sigma^{\infty}_{cr}$ is the lowest value of $\Delta\sigma_{cr}$, which is reached for very large specimen sizes. Thus, because for $b \to +\infty$ the specimen-size dependence disappears, $\Delta\sigma^{\infty}_{cr}$ represents a material constant.

5 | EXPERIMENTAL ASSESSMENT OF THE SCALING LAW FOR FATIGUE LIMIT

In this section, some experimental results on aluminium alloy flat hourglass samples[47] are considered, although geometrical self-similarity of the specimens should be required for proper comparison among specimens with the same stress concentration. Different Wöhler's curves in the power-law regime are obtained for different specimen sizes, as shown in Figure 7. When the experimental results are reported in the fractal Wöhler's diagram, they collapse onto a single straight line in the power-law regime, independently of the specimen size. The renormalization of the Wöhler's diagram yields to a scale-invariant curve.

Best-fitting of experimental data, in order to collapse them onto a single curve, provides the dimensional decrement d_σ, which is equal to 0.13 in the case of the data collected in Tomaszewsky and Sempruch.[47] Eventually, the fractal stress-range will show the anomalous physical dimensions $[F][L]^{-(1.87)}$ (see Figure 8).

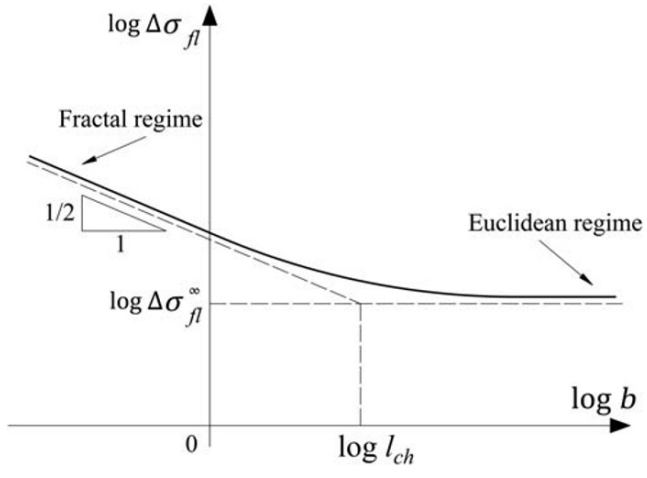

FIGURE 6 Multi-Fractal Scaling Law for fatigue limit

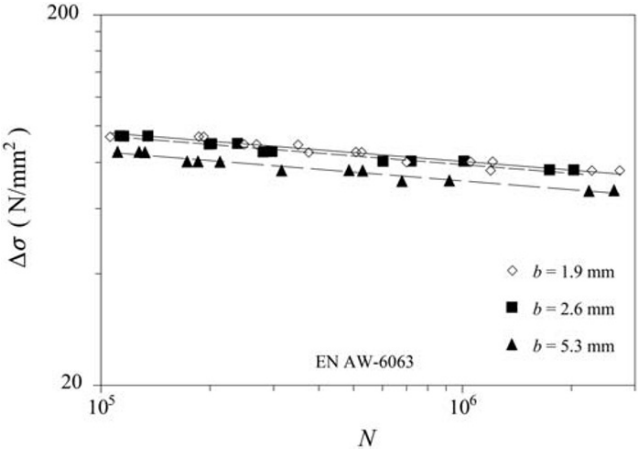

FIGURE 7 Experimental specimen-size dependent Wöhler's curves in the power-law regime for EN AW-6063[47]

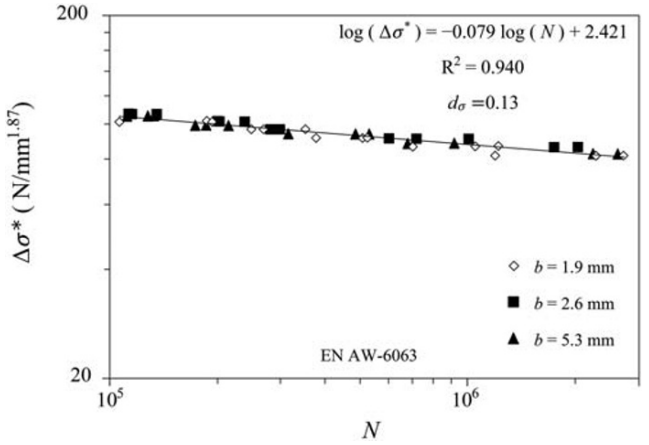

FIGURE 8 Experimental fractal Wöhler's curve in the power-law regime for EN AW-6063

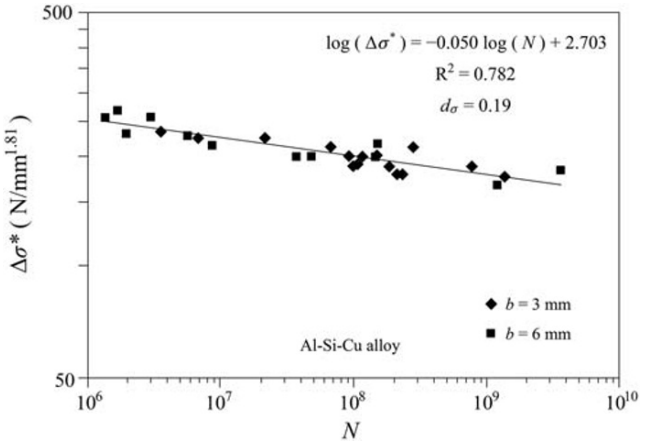

FIGURE 10 Experimental fractal Wöhler's curve for Al-Si-Cu alloy

Xue et al.[48] performed fatigue tests on Al-Si-Cu cast alloy specimens beyond 10^9 cycles with an ultrasonic fatigue testing machine operating at 20 kHz and $R = -1$. They considered hourglass specimens 3 and 6 mm in diameter at the middle cross-section. The experimental data show that, for a certain number of cycles, the larger the diameter of the ligament, the lower the fatigue strength. As a consequence, in the Wöhler's diagram of Figure 9, two different curves are obtained depending on the specimen-size. On the contrary, if the fractal Wöhler's diagram of Figure 10 is adopted, all the data collapse onto a single straight line. The physical dimensions of the fractal stress range $\Delta\sigma^*$, equal to $[F][L]^{-(1.81)}$, are obtained by best-fitting of experimental data.

In addition, in the present section, the experimental data available in the Literature are fitted with Equation 16.

Hatanaka et al. performed a set of fatigue tests to investigate the specimen-size effects on Wöhler's curve.[49]

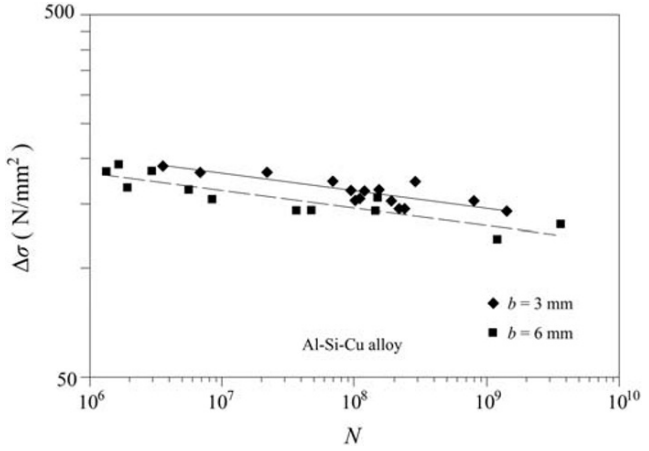

FIGURE 9 Experimental specimen-size dependent Wöhler's curves for Al-Si-Cu alloy[48]

Considering two different materials and dog-bone specimens 8, 20, 30, and 40 mm in diameter, tests were carried out through a rotating bending machine. More specifically, the two materials used are a cast steel, JIS SCMn 2A, and a forget steel, JIS SF 50. From the test results and for both materials, a decrease in the fatigue strength with the specimen size was highlighted. In particular, it was observed that, in accordance with fractal geometry, the decrement in fatigue strength was more pronounced for the material with a less homogenous microstructure, that is, JIS SCMn 2A.

Thus, by focusing our attention on the fatigue limit, a linear regression provides the best-fitting parameters entering Equation 16 for the two steel alloys. Considering SF50 steel, we obtain the following equation for the fatigue limit:

$$\log\Delta\sigma_{fl} = 2.74 - 0.08\log b, \tag{20}$$

which implies that the fractal dimension decrement is equal to 0.08, thus revealing a dimension of material ligament equal to 1.92, whereas the fractal fatigue limit, which represents the true material constant, is 279 N $mm^{-1.92}$ (see Figure 11). On the other hand, considering SCMn 2A steel, we have the following expression for the fatigue limit:

$$\log\Delta\sigma_{fl} = 2.80 - 0.16\log b, \tag{21}$$

which provides a value of the fractal dimension decrement equal to 0.16, whereas the fractal fatigue limit is 318 N $mm^{-1.84}$ (Figure 12).

Notice that the obtained values for the fractal decrement d_σ are consistent. The more ordered the material, the closer the material ligament to a two-dimensional Euclidean surface. In fact, for the SF50 steel, which is the

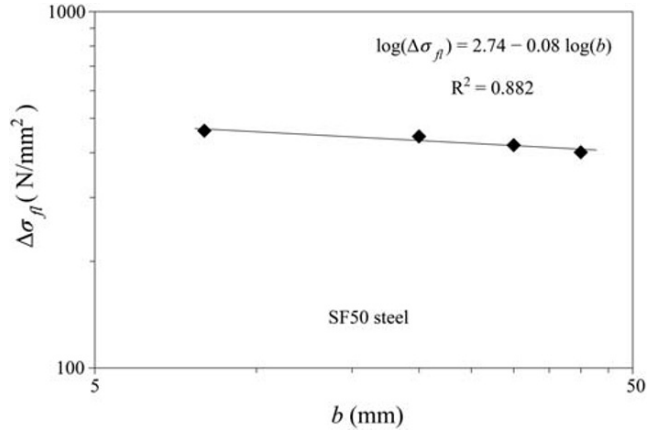

FIGURE 11 Experimental assessment of fatigue limit for SF50 steel[49]

more ordered material, the dimensional decrement of the fractal domain is smaller than that obtained for SCMn 2A.[50] Eventually, it is interesting to point out that the values obtained are always lower than 1/2, in accordance with the hypothesis of statistical crack-size distribution of self-similarity.[51]

Subsequently, we consider the experiments carried out by Furuya on specimens made up of high-strength steel, that is, JIS-SCM440 low-alloy steel, by means of an ultrasonic fatigue testing machine.[52] The experimental evidence shows that the fatigue failure, for this kind of steels, is mainly caused by fish-eye fracture, that is, an internal penny-shaped crack that is originated mostly from an inclusion.[20]

These ultrasonic fatigue tests were conducted at 20 kHz, with a stress ratio $R = -1$. Furthermore, these tests were carried out using a dog-bone specimen 8 mm in diameter and hourglass-shaped specimens 3 and 7 mm in diameter.

As in the previous case, a linear regression permits us to obtain the following relationship for the fatigue limit:

$$\log\Delta\sigma_{fl} = 3.26 - 0.16\log b, \tag{22}$$

which provides the values of the best-fitting parameters. Thus, considering Equation 22, a value of the fractal dimension decrement equal to 0.16 is expected, whereas the fractal fatigue limit is 1820 N mm$^{-1.84}$ (Figure 13).

In addition, the experimental data by Pegues et al.[53] on additively manufactured (AM) Ti-6Al-4V titanium alloy samples are analysed. In order to investigate the sensitivity of the titanium alloy to the specimen size, the authors carried out fatigue tests on dog-bone samples 3.25, 4.90, and 7.30 mm in diameter, with traditional MTS testing machine under fully reversed, $R = -1$, force control conditions, up to 10^7 cycles. The fatigue limit decreases with the specimen size, as shown in Figure 14. In order to perform the best-fitting with Equation 16, the experimental values of the fatigue limit can be plotted versus the specimen size in a bi-logarithmic diagram, which provides:

$$\log\Delta\sigma_{fl} = -0.41\log b + 2.85. \tag{23}$$

It is interesting to note that a rather high value of the fractal decrement d_σ is obtained, which is consistent with the augmented disorder of the microstructure of the considered material. In fact, according to Li et al.[54] AM titanium alloys are characterised by a high quantity of internal defects in the form of porosity and lack of fusion defects containing unmelted particles. Fatemi et al.[55] reported that the AM samples contained many spherical pores, with dimensions ranging from 5 to 80 μm, and irregularly shaped voids with size of up to 500 μm due to the lack of fusion.[56] As a consequence, AM can significantly reduce the fatigue strength of components.[57] Anyway, a dimensional decrement d_σ equal to 0.41 is less than the maximum theoretical allowed value of 0.50.

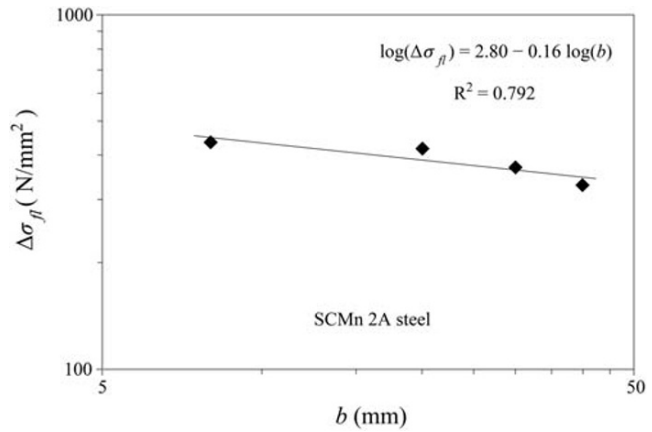

FIGURE 12 Experimental assessment of fatigue limit for SCMn 2A steel[49]

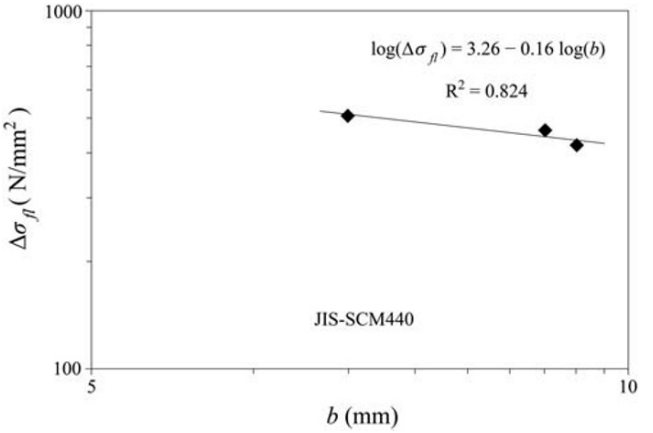

FIGURE 13 Experimental assessment of fatigue limit for JIS-SCM440 low-alloy steel[52]

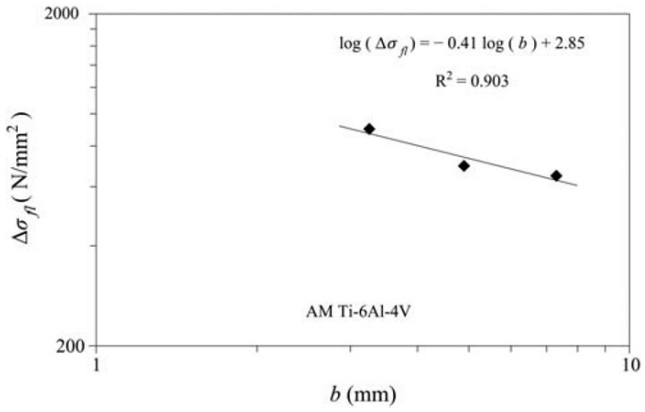

FIGURE 14 Experimental assessment of fatigue limit for AM Ti-6Al-4V[53]

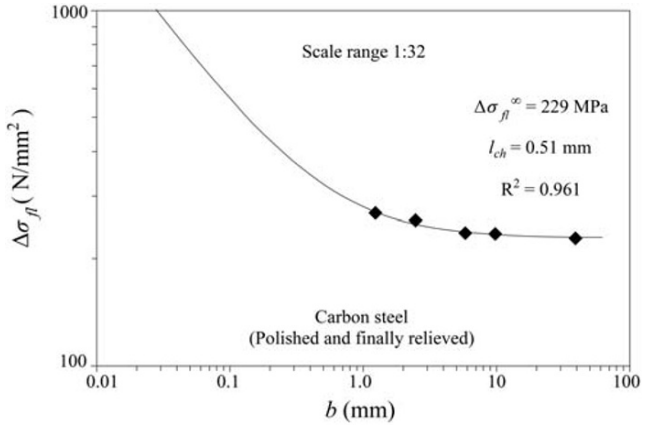

FIGURE 15 Multi-Fractal Scaling Law experimental assessment of the fatigue limit for a carbon steel (polished and finally relieved)[58]

Eventually, the experimental data set obtained by Kelly and Morrison[58] are analysed. In this experimental campaign, rotating bending fatigue tests were carried out on two sets of mild steel dog-bone specimens, covering a size range from 1.27 to 40.64 mm. The fitting with the MFSL of Equation 18 provides the asymptotic value of the fatigue limit, $\Delta\sigma^{\infty}_{fl}$, and the material characteristic length of the material, l_{ch} (see Figure 15). It is worth noting that the MFSL for the fatigue limit can properly interpolate the results obtained from a much wider scale range and that very high cycle fatigue test results could be obtained as well.

6 | CONCLUSIONS

When stress-life (S-N) approach was introduced in the 19th century, size effects were not yet known. In fact, the role of specimen size on the fatigue behaviour has been investigated only in recent times, and much effort has been made to interpret the phenomenon, which has led to the use of empirical relationships, such as the $\sqrt{area}$ model proposed by Murakami or other statistical approaches.

In this paper, dimensional analysis and intermediate asymptotics are used to find a generalised formulation for Wöhler's curve. Furthermore, by proposing a model based on the concept of lacunar fractality, the specimen-size dependence of Wöhler's curve is explained. The proposed models were compared with experimental data available in the Literature from which it follows that the fractal approach is able to explain the size effects on Wöhler's curve. Eventually, with the aim of providing a more accurate modelling, a multi-fractal approach is put forward both for fatigue limit and critical stress range.

ACKNOWLEDGEMENTS

This research did not receive any specific grant from funding agencies in the public, commercial, or not-for-profit sectors.

NOMENCLATURE

$\Delta\sigma$	stress range
$\Delta\sigma^{*}$	fractal stress range
$\Delta\sigma_0$	Basquin's parameter
$\Delta\sigma_{cr}$	critical stress range
$\Delta\sigma^{*}_{cr}$	fractal critical stress range
$\Delta\sigma^{\infty}_{cr}$	asymptotic value of the critical stress range
$\Delta\sigma_{fl}$	fatigue limit
$\Delta\sigma^{*}_{fl}$	fractal fatigue limit
$\Delta\sigma^{\infty}_{fl}$	asymptotic value of the fatigue limit
σ_u	ultimate tensile strength
σ^{*}_u	fractal ultimate tensile strength
σ^{∞}_u	asymptotic value of the ultimate tensile strength
$area$	orthogonally projected area of the defect with respect to the applied stress range
b	specimen size
d_σ	dimensional decrement of ligament area
HV	Vickers hardness
K_{IC}	fracture toughness
l_{ch}	characteristic material length
N	number of cycles
N_{cr}	number of cycles below which tensile resistance is not decreasing
N_{fl}	number of cycles beyond which fatigue resistance is not decreasing
n	exponent of Basquin's law
R	loading ratio

ORCID

Alberto Carpinteri https://orcid.org/0000-0002-5367-6560

Francesco Montagnoli https://orcid.org/0000-0002-4729-796X
Stefano Invernizzi https://orcid.org/0000-0001-6334-7931

REFERENCES

1. Wöhler A. Über die Festigkeitsversuche mit Eisen und Stahl. *Zeitschrift für Bauwesen*. 1870;20:73-106.
2. Basquin OH. The exponential law of endurance tests. *ASTM Proceedings*. 1910;10:625-630.
3. Schijve J. *Fatigue of Structures and Materials*. New York: Springer; 2009.
4. Moore RH, Harter HL. A survey of the literature on the size effect on material strength. *J Am Stat Assoc*. 1978;72:362-364.
5. Weibull W. A statistical theory for the strength of materials. *Royal Swedish Institute of Engineering Research (Ingeniöersvetenskaps Akademiens Handllingar)*. 1939;151:1-45.
6. Barenblatt GI, Botvina LR. Incomplete self-similarity of fatigue in the linear range of crack growth. *Fatigue Fract Eng Mater Struct*. 1980;3:193-202.
7. Murakami Y. *Metal Fatigue: Effects of Small Defects and Non-metallic Inclusions*. Oxford: Elsevier Science; 2002.
8. Murakami Y, Kodama S, Konuma S. Quantitative evaluation of effects of non-metallic inclusions on fatigue strength of high strength steels. I: basic fatigue mechanism and evaluation of correlation between the fatigue fracture stress and the size and location of non-metallic inclusions. *Int J Fatigue*. 1989;11:291-298.
9. Murakami Y, Usuki H. Quantitative evaluation of effects of non-metallic inclusions on fatigue strength of high strength steels. II: fatigue limit evaluation based on statistics for extreme values of inclusion size. *Int J Fatigue*. 1989;11:299-307.
10. Weibull W. A statistical representation of fatigue failures in solids. *Trans Royal Inst Technol*. 1949;27:1-49.
11. Murakami Y, Yokoyama NN, Nagata J. Mechanism of fatigue failure in ultralong life regime. *Fatigue Fract Eng Mater Struct*. 2002;25:735-746.
12. Chapetti MD, Tagawa T, Miyata T. Ultra-long cycle fatigue of high-strength carbon steels part I: review and analysis of the mechanism of failure. *Mater Sci Eng A*. 2003;356:227-235.
13. Bathias C, Paris P. *Gigacycle Fatigue in Mechanical Practise*. New York: CRC Press; 2004.
14. Zettl B, Mayer H, Stanzl-Tschegg SE, Degischer HP. Fatigue properties of aluminium foams at high numbers of cycles. *Mater Sci Eng A*. 2000;292:1-7.
15. Furuya Y. Notable size effects on very high cycle fatigue properties of high-strength steel. *Mater Sci Eng A*. 2011;528:5234-5240.
16. Tridello A, Paolino DS, Chiandussi G, Rossetto M. VHCF response of AISI H13 steel: assessment of size effects through Gaussian specimens. *Procedia Eng*. 2015;109:121-127.
17. Tridello A, Paolino DS, Chiandussi G, Rossetto M. Different inclusion contents in H13 steel: effects on VHCF response of Gaussian specimen. *Key Eng Mater*. 2016;665:49-52.
18. Tridello A, Paolino DS, Chiandussi G, Rossetto M. Comparison between dog-bone and Gaussian specimens for size effect evaluation in gigacycle fatigue. *Frattura e Integrità Strutturale*. 2013;26:49-56.
19. Paolino DS, Tridello A, Chiandussi G, Rossetto M. On specimen design for size effect evaluation in ultrasonic gigacycle fatigue testing. *Fatigue Fract Eng Mater Struct*. 2014;37:570-579.
20. Tridello A, Paolino DS, Chiandussi G, Rossetto M. VHCF strength decrement in large H13 steel specimens subjected to ESR process. *Procedia Struct Int*. 2016;2:1117-1124.
21. Carpinteri A. Scaling laws and renormalization groups for strength and toughness of disordered materials. *Int J Solids Struct*. 1994;31:291-302.
22. Carpinteri An, Spagnoli A, Vantadori S. Size effect in S-N curves: a fractal approach to finite-life fatigue strength. *Int J Fatigue*. 2009;31:927-933.
23. Carpinteri A, Paggi M. A unified interpretation of the power laws in fatigue and the analytical correlations between cyclic properties of engineering materials. *Int J Fatigue*. 2009;31:1524-1531.
24. Carpinteri A, Paggi M. Dimensional analysis and fractal modeling of fatigue crack growth. *J ASTM Int*. 2011;8:1-13.
25. Buckingham E. Model experiment and the form of empirical equations. *ASME Trans*. 1915;37:263-296.
26. Carpinteri A. Notch sensitivity in fracture testing of aggregative materials. *Eng Fract Mech*. 1982;16:467-481.
27. Barenblatt GI. *Scaling, Self-similarity and Intermediate Asymptotics*. UK: Cambridge University Press; 1996.
28. Barenblatt GI. *Scaling*. UK: Cambridge University Press; 2003.
29. Barenblatt GI. Scaling phenomena in fatigue and fracture. *Int J Fract*. 2006;138:19-35.
30. Carpinteri A, Montagnoli F. Scaling and fractality in subcritical fatigue crack growth: crack-size effects on Paris' law and fatigue threshold. *Fatigue Fract Eng Mater Struct*. 2020;43:788-801.
31. Falconer K. *Fractal Geometry: Mathematical Foundations and Applications*. Chichester: Wiley; 1990.
32. Carpinteri A. Fractal nature of material microstructure and size effects on apparent mechanical properties. *Mechanics of Materials*. 1994; 18: 89–101. Internal Report, Laboratory of Fracture Mechanics, Politecnico di Torino, N. 1/92, 1992.
33. Carpinteri A, Ferro G. Size effects on tensile fracture properties: a unified explanation based on disorder and fractality of concrete microstructure. *Mater Struct (RILEM)*. 1994;27:563-571.
34. Carpinteri A, Chiaia B. Power scaling laws and dimensional transitions in solid mechanics. *Chaos Soliton Fract*. 1996;7:1343-1364.
35. Carpinteri A, Chiaia B. Fractals, Renormalization Group Theory and Scaling Laws for Strength and Toughness of Disordered Materials. In: Breysse D, ed. *Proceedings of the workshop probabilities and materials: tests, models and applications*. Cachan, France: Kluwer Acad Publishers; 1994:141-150.
36. Carpinteri A, Chiaia B. Multifractal scaling laws in the scaling behaviour of disordered materials. *Chaos Soliton Fract*. 1997;8:135-150.
37. Carpinteri A, Chiaia B, Ferro G. Size effects on nominal tensile strength of concrete structures: multifractality of material ligaments and dimensional transition from order to disorder. *Mater Struct (RILEM)*. 1995;28:311-317.
38. Carpinteri A, Ferro G, Invernizzi S. The nominal tensile strength of disordered materials: a statistical fracture mechanics approach. *Eng Fract Mech*. 1997;58:421-435.

39. Carpinteri A, Chiaia B, Cornetti P. On the mechanics of quasi-brittle materials with a fractal microstructure. *Eng Fract Mech*. 2003;70:2321-2349.
40. Carpinteri A, Chiaia B, Cornetti P. A scale-invariant cohesive crack model for quasi-brittle materials. *Eng Fract Mech*. 2002; 69:207-217.
41. Carpinteri A, Cornetti P, Puzzi S. Scaling laws and multiscale approach in the mechanics of heterogeneous and disordered materials. *Applied Mech Rev*. 2006;59:283-305.
42. Carpinteri A, Chiaia B, Ferro G. A new explanation for size effects on the flexural strength of concrete. *Mag Concrete Res*. 1997;49:45-53.
43. Carpinteri A, Chiaia B, Ferro G. Scale dependence of tensile strength of concrete specimens: a multifractal approach. *Mag Concrete Res*. 1998;50:237-246.
44. Carpinteri A, Chiaia B. Multifractal nature of concrete fracture surfaces and size effects on nominal fracture energy. *Mater Struct (RILEM)*. 1995;28:435-443.
45. Carpinteri An, Spagnoli A, Vantadori S. An approach to size effect in fatigue of metals using fractal theories. *Fatigue Fract Eng Mater Struct*. 2002;25:619-627.
46. Montagnoli F, Invernizzi S, Carpinteri A. Fractality and size effect in fatigue damage accumulation: comparison between Paris and Wöhler perspectives. In: Carcaterra A, Paolone A, Graziani G, eds. *Proceedings of XXIV AIMETA Conference*. Rome, Italy: Lecture Notes in Mechanical Engineering; 2020: 188-196.
47. Tomaszewsky T, Sempruch J. Analysis of size effect in high-cycle fatigue for EN AW-6063. *Solid State Pheno*. 2015;224: 75-80.
48. Xue H, Sun Z, Zhang X, Gao T, Li Z. Very high cycle fatigue of cast aluminium alloy: size effect and crack initiation. *J Mater Eng Perf*. 2018;27:5406-5416.
49. Hatanaka K, Shimizu S, Nagae A. Size effect on rotating bending fatigue in steels. *Bulletin of the JSME*. 1983;26:1288-1295.
50. Carpinteri A, Montagnoli F. Scaling and fractality in fatigue crack growth: implications to Paris' law and Wöhler's curve. *Procedia Struct Int*. 2019;14:957-963.
51. Carpinteri A. *Mechanical Damage and Crack Growth in Concrete: Plastic Collapse to Brittle Fracture*. Dordrecht: Martinus Nijhoff Publishers; 1986.
52. Furuya Y. Size effects in gigacycle fatigue of high-strength steel under ultrasonic fatigue testing. *Procedia Eng*. 2010;2: 485-490.
53. Pegues J, Roach M, Williamson RS, Shamsaei N. Volume effects on the fatigue behavior of additively manufactured Ti-6Al-4V Parts. In: Bourell DL, Beaman JJ, Crawford RH, Fish S, Seepersad FS, eds. *Proceedings of the 29th Annual International Solid Freeform Fabrication Symposium—An Additive Manufacturing Conference*. Austin, USA: University of Texas at Austin; 2018:1373-1381.
54. Li P, Warner D, Fatemi A, Phan N. Critical assessment of the fatigue performance of additively manufacturing Ti-6Al-4V and perspective for future research. *Int J Fatigue*. 2016;85:130-143.
55. Fatemi A, Molaei R, Sharifimehr S, Phan N, Shamsaei N. Multiaxial fatigue behavior of wrought and additive manufactured Ti-6Al-4V including surface finish effect. *Int J Fatigue*. 2017; 100:347-366.
56. Fatemi A, Molaei R, Sharifimehr S, Shamsaei N, Phan N. Torsional fatigue behavior of wrought and additive manufactured Ti-6Al-4V by powder bed fusion including surface finish effect. *Int J Fatigue*. 2017;99:187-201.
57. Fatemi A, Molaei R, Simsiriwong J, et al. Fatigue behaviour of additive manufactured materials: an overview of some recent experimental studies on Ti-6Al-4V considering various processing and loading direction effects. *Fatigue Fract Eng Mater Struct*. 2019;42:991-1009.
58. Kelly DA, Morrison JLM. Effect of specimen size and preparation on the fatigue strength of a plain carbon steel tested in rotating bending and in torsion. *Proc Institution Mech Eng*. 1970;185:655-664.

How to cite this article: Carpinteri A, Montagnoli F, Invernizzi S. Scaling and fractality in fatigue resistance: Specimen-size effects on Wöhler's curve and fatigue limit. *Fatigue Fract Eng Mater Struct*. 2020;43:1869–1879. https://doi.org/10.1111/ffe.13242